Earth Surface Processes and Landforms
Earth Surf. Process. Landforms **25**, 535–557 (2000)

IDENTIFYING LARGE-SCALE EROSION AND DEPOSITION PROCESSES FROM AIRBORNE GAMMA RADIOMETRICS AND DIGITAL ELEVATION MODELS IN A WEATHERED LANDSCAPE

GEOFF PICKUP* AND ALAN MARKS
CSIRO Land and Water, PO Box 1666, Canberra, ACT 2601, Australia

Received 15 April 1999; Revised 27 October 1999; Accepted 25 November 1999

ABSTRACT

Patterns of erosion and deposition are difficult to identify and measure at catchment and regional scale but it may be possible to infer their distribution from remote sensing using easily measured surrogate variables. Airborne geophysical surveys provide data on gamma ray emissions from surface and near-surface material and allow estimation of K, Th and U content. Gamma ray signatures are largely determined by lithology but also change with weathering and with erosion and deposition, and may be used as a partial surrogate for those processes. Comparison of gamma ray signatures with topographic characteristics closely related to sediment transport capacity, downstream sorting of sediments, and the extent of erosion and deposition shows strong linkages. Studies in four small catchments in southeastern Australia indicate that K consistently increases as slopes become steeper while Th and U may either increase or decrease. This suggests the presence of fresh rock rather than weathered material and implies removal of material by erosion, although some patterns may result from systematic changes in lithology across catchments. Analysis by lithology confirms the increase in K with slope in granites, metamorphosed sediments and basalt, and also shows a tendency for U to decrease with slope in the granites and basalt. Gamma ray emissions vary only slightly with catchment area (a surrogate measure of water discharge) suggesting that water erosion is limited or that discharge is not closely related to area. Gamma radiometric profiles down hillslopes, averaged across the full range of gradients, show that, in most cases, radioelements initially decrease, probably reflecting increased weathering, but then increase close to valley floors because of accumulation of fine sediments. Analysis by lithology confirms the increase in radioelements close to valley floors in granites and metamorphosed sediments but the trend is less clear in basalt. Gamma ray profiles down floodplains are variable and indicate the amount of deposition and accumulation of weathered material in valley openings and exposure of bedrock in valley constrictions. Simple erosion and deposition models, based on the conservation of mass equation, and applied to the four catchments, show that all radioelements increase as the potential for deposition increases. They reach a low point in zones of no net erosion or deposition and subsequently increase as erosion becomes more intense and weathered material is lost from slopes. Analysis by lithology largely confirms this pattern. The usefulness of airborne geophysical survey data is limited by flight line spacing with most data being flown at a 200–400 m spacing in Australia. However, general trends in erosion and deposition can still be distinguished and there is capacity for calibrating long-term erosion and deposition models once better approaches to interpretation of gamma ray data have been developed. Copyright © 2000 John Wiley & Sons, Ltd.

KEY WORDS: erosion models; gamma radiometrics; remote sensing; gradient analysis; weathered landscapes; southeastern Australia

INTRODUCTION

While considerable progress has been made in measuring and modelling erosion, transport and deposition at plot and small catchment scales (e.g. Anderson, 1988; Willgoose *et al.*, 1991; Flanagan and Nearing, 1995), major obstacles remain in scaling this work up to larger catchments and to whole regions (e.g. Walling, 1983). The most critical of these obstacles is lack of ability to measure spatially distributed, regional-scale sedimentation processes, making it difficult to identify sediment sources and sinks and therefore to verify model predictions. There is a particular need for such measurements where sediment transport is supply-limited and where the supply of sediment is governed by biological processes as well as hydrology and hydraulics (e.g. Pickup and Chewings, 1996). Existing models do not have this capacity.

* Correspondence to: Dr G. Pickup, CSIRO Land and Water, PO Box 1666, Canberra, ACT 2601, Australia

Three approaches have been used to measure erosion and sediment yield. These are:

- small plot studies in which runoff and sediment output from particular types of land cover or treatments are monitored (e.g. Nearing *et al.*, 1990; Wasson *et al.*, 1996);
- suspended sediment sampling programmes at river gauging stations (e.g. Loughran, 1984; Rieger and Olive, 1988); and
- reconstructions of erosion and deposition from sediment deposits at representative locations in the landscape using radioisotope analysis, or sediment magnetic or geochemical properties (e.g. Ritchie and McHenry, 1990; Caitcheon, 1993; Olley *et al.*, 1993; Wallbrink *et al.*, 1998).

The erosion plot measurements are usually not representative of larger areas because of local variability (e.g. Kirkby *et al.*, 1996; Croke *et al.*, in press) and inferences made about landscape processes from such samples often cannot be generalized. The gauging station data are expensive to acquire and contain aggregated information about upstream processes that cannot be easily disaggregated into behaviour in different parts of the drainage basin. Also, it may take many years before useful information can be obtained from stream gauging programmes because of variability in both flow and sediment supply. The radioisotope methods offer potential for historical reconstruction of erosion processes but provide data on individual points in the landscape at relatively high unit cost. This makes it difficult to apply them over large areas because of the large number of samples required to give a regional picture. Also, in depositional areas they provide data that are an average of upstream processes and not easy to disaggregate into behaviour of individual upstream subcatchments. Sediment magnetic properties offer more potential for disaggregation but, once again, suffer from the limitations imposed by having to extrapolate from point samples to the wider landscape. It may also be difficult to transform data into quantitative data on erosion rates in different parts of the catchment (e.g. Walden *et al.*, 1997).

While direct measurements of distributed regional-scale sedimentation processes have not proved possible, attempts have been made to model relative rates of activity using surrogate measures. For example, Pickup and Chewings (1986, 1996) used vegetation cover in rangelands to identify regional patterns in sediment gain and sediment loss. They then attempted to model those patterns using random field techniques and process descriptions of the spatial behaviour of grazing animals. Some success was achieved in predicting observed patterns of change over time but the methods do not adapt to more humid areas and to steeper terrain. Other attempts to model at the regional scale have used simple theoretical models of hillslope processes but have operated at geological time scales and cannot be checked for accuracy (e.g. Kirkby, 1995).

This paper pursues the surrogate approach further and examines how gamma ray data obtained during airborne geophysical surveys might be used to infer the relative distribution of erosion and deposition in small catchments. It begins with brief descriptions of how gamma ray data are collected from aircraft, the relationship between gamma ray signatures, and the properties of the underlying rock and regolith. A methodology for identifying the particular spatial patterns associated with erosion and deposition is described and applied to gamma ray data from small drainage basins in southeastern Australia. A short review of digital elevation model (DEM) generation from geophysical survey data is also presented since this may be a substitute for a more conventional approach in which DEMs are generated from contour data derived by photogrammetry. The paper concludes with a brief review of what is needed to make more effective use of gamma ray data.

METHODS

Airborne gamma ray spectrometry

Airborne geophysical surveys are widely used for mineral and petroleum exploration and for geological mapping. Typically, these surveys are carried out by low-flying aircraft and collect information on the magnetic properties and gamma ray emissions of underlying terrain along a series of closely spaced flight lines (Horsfall, 1997; Minty, 1997). Flight line data are then gridded using techniques described by Luyendyk

(1997) and can be analysed using a GIS or image processing system. Gamma ray data are particularly useful for distinguishing the geochemical characteristics of soils and near-surface rock types, particularly when combined with supplementary information on landscape topography (e.g. Bierworth, 1996; Cook *et al.*, 1996; Wilford *et al.*, 1997). Magnetic data, when suitably processed, provide information on geological structure (Clarke, 1997). Gamma ray data have also been used as surrogates for a variety of soil properties and processes such as acidity, aluminium toxicity, silt-clay content and areas of groundwater discharge (e.g. Bierworth, 1996). By 1996, over 20 per cent of Australia had been covered by airborne geophysical surveys with flight line spacings of 500 m or less (Denham, 1997) and the surveyed area continues to grow, providing an important database for geomorphic as well as geological studies.

Gamma ray surveys detect the abundance of potassium (K), thorium (Th) and uranium (U). These are the only naturally occurring radioisotopes with gamma ray emissions of sufficient energy and intensity to be detected by scintillation counters at the altitudes typically flown by survey aircraft. Relative K abundance is measured directly using the decay of the unstable isotope, ^{40}K at 1·46 MeV. Relative U and Th abundance are measured indirectly from the gamma-emitting daughter products, ^{214}Bi and ^{208}Tl respectively (Grasty, 1979). Relative values may be converted to absolute amounts by calibration procedures (see below). K data are then expressed as the percentage of total potassium in the surface material. U and Th data are expressed in ppm and as gamma equivalent values of uranium and thorium (eU and eTh) in surface material assuming that they are in secular equilibrium with their respective daughter products. Most of the radiation is derived from shallow depths with approximately 90 per cent coming from the top 30–45 cm for dry material with a density of 1·5g cm^{-3} (Grasty, 1975). Measured count rate declines exponentially with distance from the sensor and varies with aircraft height, forward velocity and sensor integration time. Thus, the signal recorded is a complex spatial average (Grasty, 1979) with approximately two-thirds of measured radiation coming from a circle with a diameter equal to the flying height (Dickson and Scott, 1992).

Gamma ray responses are largely determined by the geochemistry of the parent rock type and, to a lesser degree, the extent of weathering. Sediment transport and sorting may also play a role but transported sediments will still reflect the characteristics of their parent material to some extent. Other factors affecting response include soil- or surface-water, which attenuates gamma ray responses. Attenuation by vegetation is minimal except where there are dense stands of forest (Dickson and Scott, 1992). In these forested areas, reductions in gamma ray counts of 14–22 per cent have been recorded (Aspin and Bierworth, 1997).

Radio-element concentrations vary between minerals and rock types and their weathering products (e.g. Galbraith and Saunders, 1983; Dickson and Scott, 1992, 1997; Wilford, 1995). During weathering, radioelement concentrations are modified from those of the original bedrock material. K is geochemically mobile and is soluble under most weathering conditions, resulting in either loss in solution or adsorption onto clay minerals such as illite, montmorillonite and, to a lesser extent, kaolinite. U is readily leached and can be released from soluble materials under oxidizing conditions and precipitates under reducing conditions. Surface concentrations of U can be associated with resistate minerals such as zircon, or derived from ^{226}Ra associated with surface discharge of groundwater. Weathering can result in major loss of K, little effect on U, and concentration of Th by factors up to 10, depending on the underlying rock type. U and Th derived from weathering are readily adsorbed on to clay minerals, iron oxides and soil organic matter. Thus, lateritic weathering of shales can result in almost complete loss of K with little effect on U and Th (Dickson and Scott, 1992).

Differential rates of weathering may lead to variations in the gamma ray signatures of different particle size fractions in a soil profile. For example, radioelement analysis of size fractions from soils collected over granitic rocks show that U and Th tend to be retained in clay-rich or iron oxide-rich fractions (e.g. Bierworth, 1996). K concentrations are greater in coarser factions where feldspar or biotite are present (Dickson and Scott, 1992). Differential transport and deposition of individual size fractions may therefore affect gamma signatures in both erosional and depositional areas.

Some progress has been made recently in inferring patterns and relative rates of both weathering and erosion from gamma ray imagery (Wilford *et al.*, 1997). Indeed, Wilford (1995) has proposed a model in which regolith thickness at any one site depends on the relative rates of accumulation and erosion. Where weathering is more rapid than erosion, regolith thickness increases, whereas in situations where weathering

and erosion rates are similar, there will be a thin, permanently youthful regolith. Thus, in areas of erosion, gamma ray responses reflect the geochemistry and mineralogy of the bedrock, while in areas of sediment accumulation, responses are modified by pedogenesis and sorting. In the case of weathered granitic rocks, where the regolith is *in-situ*, thin partly weathered profiles on steep slopes show high K. Where rates of weathering exceed rates of erosion, for example on lower slopes, a decrease in K concentrations occurs as K-bearing minerals are progressively leached from the weathered material. Obviously, the patterns that occur in the granitic terrain may not translate directly to other rock types, but the same principle applies, and there may be other characteristic variations in gamma ray signature with slope.

It is also possible to use gamma ray responses of sediments derived from locations with particular geochemical characteristics but transported and deposited elsewhere to track the path of material across the landscape. Dickson and Scott (1992) describe how rivers and major streams show the signature of headwater rocks for considerable distances downstream. In their examples, watercourses show a K-rich response due to retention of K-bearing coarser grained materials and the loss of U- and Th-bearing finer fractions and iron oxides. Similarly, Wilford (1995) describes an example in which recently deposited channel sands sourced from mixed granitic and metamorphic provinces have high K, Th and U values closely resembling the chemistry of the bedrock source. The similarity suggests that erosion, transportation and deposition of these sediments was relatively rapid, with insufficient time for weathering to change the radioelement composition of the transported material. This implies an ability to determine relative rates of depositional activity.

Gamma ray signatures, by themselves, do not provide unequivocal information on patterns of erosion and deposition. For example, as clays accumulate in sediment sinks, gamma ray responses may become stronger. As weathered material is stripped from hillsides by erosion, fresh rock may be exposed and, in granitic terrain, this may also increase the gamma ray response. Erosion and deposition may therefore have similar signatures for a given underlying rock type. An additional complication is imposed when geology varies across a catchment or down a hillslope, confounding the already complex patterns imposed by variations in weathering and erosion and deposition. Converting the spatial patterns in gamma radiometric images to maps of erosion and deposition or regolith depth therefore requires ancillary information on terrain and on the spatial patterns common to particular geomorphic processes. We approach this problem using techniques described in the next section.

Processing of gamma ray data

Airborne gamma ray survey data, flown at 200 m line spacing, were acquired from the Australian Geological Survey Organisation. Multichannel processing techniques based on the noise adjusted singular value decomposition technique (Minty and MacFadden, 1998) were applied to the full 256-channel spectrum from the survey instrument. This approach provides substantially improved estimates of relative radiometric concentration, particularly in the U and Th channels. Prior to this, data from the U channel were largely unusable because of the low signal to noise ratio. Data were then calibrated and corrected using the processing techniques described by Grasty and Minty (1995) and Minty *et al.* (1997) for standard four channel data. These procedures are as follows:

- the normalized spectrum is corrected for instrument deadtime;
- the energy calibrated spectrum is stretched or contracted so that the peaks corresponding to the IAEA standard windows have standard channel numbers;
- aircraft, cosmic and radon background signals are removed from the spectrum;
- signals are stripped to remove overlap in the spectral windows for each radioelement, height-corrected, and adjusted to ground concentrations.

It may also be useful to apply correction factors which allow for elevation differences within the sensor footprint where terrain is extremely rugged (Schwarz *et al.*, 1992). However, this is not standard practice or considered necessary in most of Australia.

The height correction and sensor calibration coefficients are derived by flying transects over a calibration range with known ground concentrations. This allows conversion of sensor counts per second to absolute

radioelement concentration. Several heights are flown to assess changes in sensor performance with altitude above ground level.

Final steps in processing involved microlevelling and resampling to a grid spacing of 100 m. This is larger than the industry standard where data are routinely gridded to one-third or one-quarter of flight line spacing. However, given that we use first and second derivatives of the DEM in the erosion model spatial templates (see below), this spacing was selected to minimize the artifacts generated by interpolation routines used in DEM generation.

Gradient analysis and spatial templates

While progress has been made in relating gamma ray responses to relative rates of erosion and deposition, the linkage has usually been made by recognizing distinctive spatial patterns by eye after draping gamma ray images over DEMs. However, while this approach may work with patterns that are fairly obvious, it may not be suitable for more complex situations where a range of weathering and sediment redistribution processes are at work. It may also be unsuitable where the underlying geology is complex, or where there is significant noise in the gamma ray data. Furthermore, introduced material may enrich the radioelements of a soil, add a radioelement-poor dilutant, or leave the radioelement content of the *in-situ* soil unchanged (Dickson and Scott, 1992). Consequently, no single pattern of change in the downslope direction is symptomatic of downslope transport. More sophisticated pattern analysis techniques may be needed to extract and interpret the spatial variations in gamma ray signatures associated with transport and deposition.

One approach to pattern extraction is to use models of the geomorphic processes which generate spatial patterns in the landscape. These patterns may then be compared with spatial structures in the gamma ray data. Analysis of residuals between generated patterns and observed data can be useful when looking for additional pattern-generating processes. Also, spatial patterns in residuals may show where particular geomorphic processes do not occur or do not have sufficient influence to generate a pattern in the gamma ray data. Pickup and Chewings (1994, 1996) used this approach to test the effectiveness of erosion models and to separate land degradation from other sources of variation in multitemporal Landsat MSS data. It was also used by Dickson *et al.* (1996) to predict the distribution of radioelements on the basis of a regression relationship between an erosion model based on the Universal Soil Loss Equation (Wischmeier and Smith, 1978) and observed gamma ray values.

Our approach to spatial pattern recognition and extraction is to generate a series of templates that describe spatial patterns in the landscape resulting from particular geomorphic processes. For example, analysis of a DEM may produce a map of slope which is a major determinant of sediment transport rate. We then compare slopes with gamma ray values to see whether an association exists between steepness and radioelement concentration. Where this is the case, we might then infer that radioelement distribution varies with sediment transport rate if other potential causes can be eliminated.

The geomorphic process templates used here consist of generated maps that describe:

- spatial variations in rates of sediment transport calculated as functions of slope and upstream drainage area;
- spatial patterns of erosion or deposition based on solutions of the conservation of mass equation; and
- downstream patterns of sediment sorting based on distance upstream or downstream.

The spatial templates are derived from analysis of DEMs and the sediment transport equations described later in this section. Initially, a DEM is constructed from the radar altimeter and differential global positioning system data obtained during the airborne survey (see below) or from pre-existing contour data. In this paper, we have used the airborne survey data and generated a DEM with a grid cell size of 100 m from flight lines spaced 200 m apart. Standard terrain analysis routines are then used to remove pits, to calculate slope and aspect, to identify flow paths, and to determine the upslope area draining into each grid cell. Subcatchment boundaries may also be determined and the distance from the catchment outlet calculated for each grid cell. Several terrain analysis packages provide this functionality including the Digital Relief Model (DRM) of Bauer (1988) which is used here.

The geomorphic process templates are compared with gamma radiometric data using gradient analysis (Pickup and Chewings, 1994). Gradient analysis involves grouping the values in each spatial template image into discrete classes and overlaying them on a georeferenced gamma radiometric image. The mean value and variance in each channel of the gamma ray image associated with each class in the spatial template image is then calculated. The technique is analogous to a simple cross-plot of two image channels but has the advantage that most of the variation is filtered out. This makes it possible to identify quite complex relationships between variables, which would be otherwise obscured by noise when every pixel is plotted against its counterpart value in the other image.

Where gradient analysis shows that spatial patterns in the gamma ray data match the process templates, it is possible that the gamma ray patterns result from a process similar to that used to generate the spatial template. They might also result from some other factor that is correlated with the process template, creating a spurious relationship. For example, steep headwater regions and flatter valley areas might occur in different rock types, creating a spurious relationship between gamma radiometric values and slope. However, if spurious alternatives can be eliminated, confidence in geomorphic explanations for particular spatial patterns increases substantially. We therefore examine patterns in individual catchments (where spurious relationships may result from downstream changes in lithology) and by lithology (where the spurious effects may come from systematic downstream variations in sediment transport and sorting). If an association between a spatial process template and gamma ray data persists both within catchments and within particular lithologies, it is less likely to be spurious.

Three sediment transport relationships (see Kirkby, 1987) and associated solutions of the conservation of mass equation are used to generate spatial templates. On hillslopes, where sediment transport is by soil creep and rainsplash, and the transport rate is proportional to slope, then:

$$g = -kS \tag{1}$$

$$\frac{\partial z}{\partial t} = k\left[\frac{\partial^2 z}{\partial x^2} + \frac{\partial^2 z}{\partial y^2}\right] \tag{2}$$

where g is the sediment transport rate by volume, z is elevation, t is time, S is slope in the direction of flow, and k is a constant. This assumes that source and sink terms in the conservation of mass equation are small enough to be ignored for practical purposes. A variation on this model is to have the transport rate as a power function of slope. Thus:

$$g = -kS^b \tag{3}$$

$$\frac{\partial z}{\partial t} = k\left[\frac{\partial}{\partial x}\left(S^{b-1}\frac{\partial z}{\partial x}\right) + \frac{\partial z}{\partial y}\left(S^{b-1}\frac{\partial z}{\partial y}\right)\right] \tag{4}$$

A transport model based on water erosion has the transport rate as a power function of slope and discharge. Since discharge is a power function of catchment area (e.g. Grayson *et al.*, 1996), the transport rate and solution to the conservation of mass equation are:

$$g = -kS^bA^c \tag{5}$$

$$\frac{\partial z}{\partial t} = k\left[\frac{\partial}{\partial x}\left(S^{b-1}A^c\frac{\partial z}{\partial x}\right) + \frac{\partial}{\partial y}\left(S^{b-1}A^c\frac{\partial z}{\partial y}\right)\right] \tag{6}$$

where A is catchment area per unit of contour length.

In less steep terrain such as river valleys, the flow is subject to downstream control and it may be necessary to solve the gradually varied flow equation (Chow, 1959) to determine the hydraulic parameters which affect

the rate of sediment transport. Our algorithm for applying this approach to a DEM is as follows. Firstly, upstream drainage area is calculated for all locations in the landscape. A minimum drainage area criterion is set and drainage channels are located in the thalweg for areas greater than this. Channel location data are then sorted into increasing order of elevation and a discharge of a particular frequency is determined at each location as power function of drainage area. The next step is to determine flow cross-sections at each point along the drainage channel. This is done by constructing a line orthogonal to the steepest direction of flow at each drainage channel location and determining the elevations at a series of distance steps equivalent to one DEM grid cell from the channel along the orthogonal. Given these data on discharge and drainage channel characteristics, a flow profile can be constructed using the standard step method for gradually varied flow analysis. The relevant hydraulic parameters for estimation of sediment transport capacity are calculated as part of this process. Values of the hydraulic parameters for areas between cross-sections are interpolated.

Downstream sorting templates use distance from catchment outlet and distance from floodplain as location measures when searching for downslope or downstream trends in gamma ray data. These templates are normally used in association with landscape masks and can be applied to separate out different landscape types. In this paper, we have applied the gradually varied flow algorithm with an extreme flow event to identify the location of valley floors in catchments with areas greater than 1 km^2. This provides a spatial mask that separates the landscape into 'floodplains' or main valley floors and 'hillslopes' comprising hillsides, crests and relatively steep, low order streams.

DEM Generation and quality

The validity of the spatial templates is heavily dependent on the quality of the DEM data from which they were derived. Highly accurate elevation data for large areas are difficult to obtain in Australia unless a specialized mapping exercise has been undertaken. Most DEMs therefore must be derived from digitized contour information and spot heights from topographic maps. Contour intervals of 20 m or more are standard. This means that, while reasonably good information is sometimes available for the steeper parts of the landscape, areas with gentle slopes, such as floodplains, are poorly described. Also, when contour information is sparse, DEM generation involves interpolation across many grid cells and can produce artifacts. These artifacts distort slopes and flowpaths and may result in highly inaccurate drainage networks.

An alternative to generating DEMs from contours is to produce them from data collected during geophysical survey. Information on terrain elevation may be derived from the aircraft's radar altimeter in combination with the aircraft-mounted differential global positioning system. Horsfall (1997) states that errors in elevation from currently used systems are 3 m or less, while R. Brodie of the Australian Geological Survey Organisation (pers. comm.) reports that 90 per cent of line data are accurate to within 2 m when checked against surveyed elevations of gravity measurement stations. Also, tests in savanna landscapes show that the radar data penetrate tree canopies sufficiently to produce ground rather than treetop elevations and so may give better DEMs than elevations derived by photogrammetry under some circumstances (Ong and Hick, 1998). While 2–3 m accuracy cannot be expected once additional errors are introduced, when line data are interpolated to a DEM grid, results are still good. For example, our experiments on the floodplain areas of central Australia show that DEMs derived from geophysical data with a line spacing as great as 400 m provide a better reproduction of patterns of water flow and flooding than DEMs based on 20 m contour data from 1:100 000 topographic maps. Comparison of mapped drainage lines with those generated from DEMs based on geophysical survey data also yields good results for flat areas but declines in accuracy in more rugged terrain where the line spacing is too great to capture all the topographic variations. In this case, the contour data are superior. (G. Pickup and A. Marks, paper submitted for publication in *Earth Surface Processes and Landforms*, 1999).

STUDY AREA CHARACTERISTICS

We have applied the gradient analysis and spatial template methodology to a 980 km^2 area of the Southern and Central Highlands Fold Belt near Goulburn, New South Wales in Australia's Southern Highlands (Figure 1). The area has average annual rainfalls of 600–850 mm and monthly mean temperatures ranging from 6·2°C

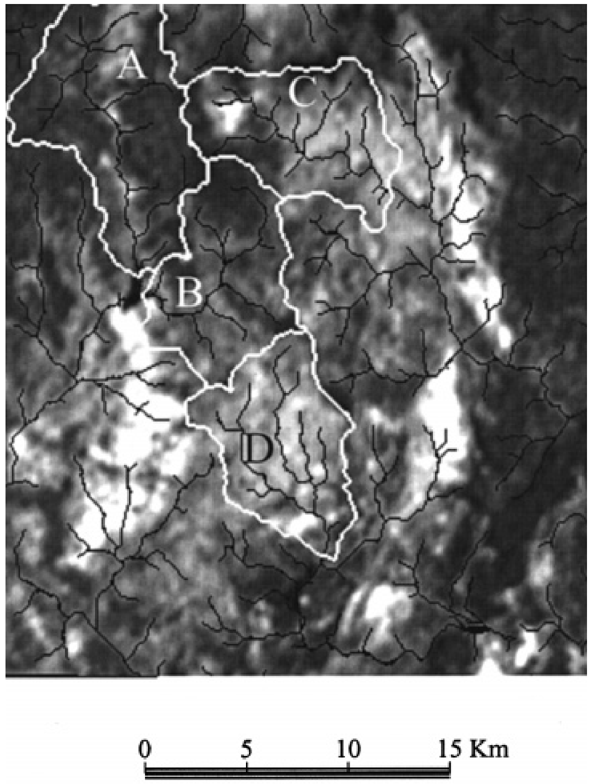

Figure 1. Grey-scale image of K values with catchment boundaries (white) and main drainage lines (black) superimposed. A is the Wollondilly River, B is Pejar Creek, C is Tarlo Creek and D is Sooley Creek (North)

in the coldest month to 19·9°C in the hottest month. The terrain is heavily dissected and the gamma ray data show mainly geological influences with some lesser weathering effects. Three major lithologies are present: granite, basalt and metamorphosed sediments. Each has a characteristic and different radioelement and weathering pattern (B. Dickson, pers. comm.). The granite appears zoned with a radioelement-rich core and a more potassic rim. Weathering of this felsic rock will lead to some but not great loss in all three radioelements. The metamorphosed sediments will probably not change their radioelement contents much during weathering. The basalts weather to form soils with low K but elevated Th and moderate U. Another factor affecting radioelement patterns is that clays tend to have higher U and Th contents than coarse material and source rocks, so sorting should produce changes in radioelement contents (Olley, 1994).

Soil profiles show extensive weathering and leaching due to both past and present climatic effects (Hird, 1991). Soil surface textures appear to be determined by parent rock but there has been extensive erosion and deposition in the past, affecting both soil profile development and soil depth. Sediment transport processes are not very active at present although clearing of native woodland has increased erosion in some areas. On ridge crests, Lithosols and Shallow Earths occur almost irrespective of the nature of the parent rock. On hillslopes and footslopes, there are extensive colluvial and fan deposits, with Red and Yellow Podzolic Soils and Soloths on the more siliceous rocks (such as granite, sandstone and shale). Red and Yellow Earths on hillslopes are associated with the less siliceous rocks (such as tuffs and andesites). Krasnozems, Prairie Soils and Chocolate Soils have formed on moderately weathered basaltic rocks in the northern part of the area (Hird, 1991).

We have taken two approaches to detection of erosion and deposition patterns in the gamma radiometric data. Firstly, four catchments, with areas of 40–80 km^2, have been examined to identify whether spatial patterns in gamma ray data are similar to those generated from the geomorphic process templates. Secondly,

we have stratified the data by lithology to see whether these patterns persist across catchments. This should identify spurious associations. The lithological stratification was done from the Goulburn 1:250 000 geology map (Felton, 1974), with detail from soil landscape mapping (Hird, 1991). Only areas that clearly fall into one or other of the three major lithological types were used and mixed environments were avoided.

The catchments have been segmented into slopes and floodplains. This allows separation of adjacent areas with different sediment source areas or different depositional and weathering histories. Identification of floodplains was carried out using a gradually varied flow analysis (see above) and assigning those areas covered by floodwater as floodplains. Areas not occupied by floodplains were classified as hillslopes. The separation of floodplains from hillslopes compares favourably with topographic map data.

The topographic characteristics of the catchments are illustrated by variation in mean floodplain elevation with distance from the lower end of each catchment (Figure 2a and c) and the frequency distribution of elevations (Figure 2b and d). The irregularities in long profile occur because mean floodplain elevation is plotted rather than elevation of the thalweg and indicate the presence of either constrictions (higher mean floodplain elevation) or openings (lower mean floodplain elevation). Knowing the location of constrictions is useful in identifying areas where deposited and weathered material is unlikely to have accumulated because flow velocities are relatively high. Conversely, openings usually represent areas of reduced sediment transport capacity and likely accumulation of deposited and weathered material. The frequency distribution of elevations in each catchment provides a measure of terrain ruggedness and topographic shape.

The individual catchments were selected to provide a range of geological types and topographies. Pejar Creek drains metamorphosed shales, but with smaller areas of basalt and dolerite, and exposures of weathered granite close to the catchment outlet into Pejar Dam. The floodplain elevations indicate a relatively smooth, concave-upward long profile with few irregularities except at the downstream end of the catchment. The frequency distribution of elevations is narrow and skewed to the left suggesting a gently sloping catchment with well-developed plains at lower elevations. The Wollondilly River is more diverse, with basalt dykes on hilltops and basalt-derived valley fills in the northern part of the catchment, whereas the southern part has weathered granite on hillslopes and fresh granite close to the river. The floodplain elevations show a concave-upward long profile in the upper part of the catchment with a steepened section downstream marked by considerable irregularities. The steepened section indicates a wave of erosion moving upstream and the irregularities are associated with rock bars and valley openings. The frequency distribution of elevations indicates that much of the catchment consists of a plateau that is dissected by steep and relatively narrow valleys. The catchment of Sooley Creek (North) is largely composed of Ordovician metasediments, although there are smaller areas of Silurian greywacke and slate. The frequency distribution of elevations is typical of a steep well-dissected catchment while floodplain elevations show two concave-upward elements and a number of valley constrictions and openings. Tarlo Creek has a diverse geology with basaltic rocks, Silurian and Ordovician sedimentaries, and granitic rocks that have weathered into a wide range of soil types. The frequency distribution of elevations indicates a plateau that has been heavily dissected, with steep slopes throughout. Floodplain elevations show a steep concave-upward profile with irregularities in the lower part of the catchment and a gentler long profile further upstream.

RESULTS

Gamma radiometric patterns on hillslopes

Inferences about the form of sediment transport relationships on hillslopes may be made through gradient analysis of gamma radiometric variables using slope and drainage area (a surrogate for water discharge) as process templates as long as fresh rock and deposited/weathered material have different gamma ray signatures. The assumption here is that areas with high sediment transport rates will not accumulate deposited material and will have gamma ray signatures more characteristic of fresh rock than of deposited and weathered material. Conversely, areas with low sediment transport rates are more likely to be mantled by deposited and weathered material and will have a different gamma ray signature. These differences may be confounded by systematic geological differences between areas with steep and gentle slopes. They may also

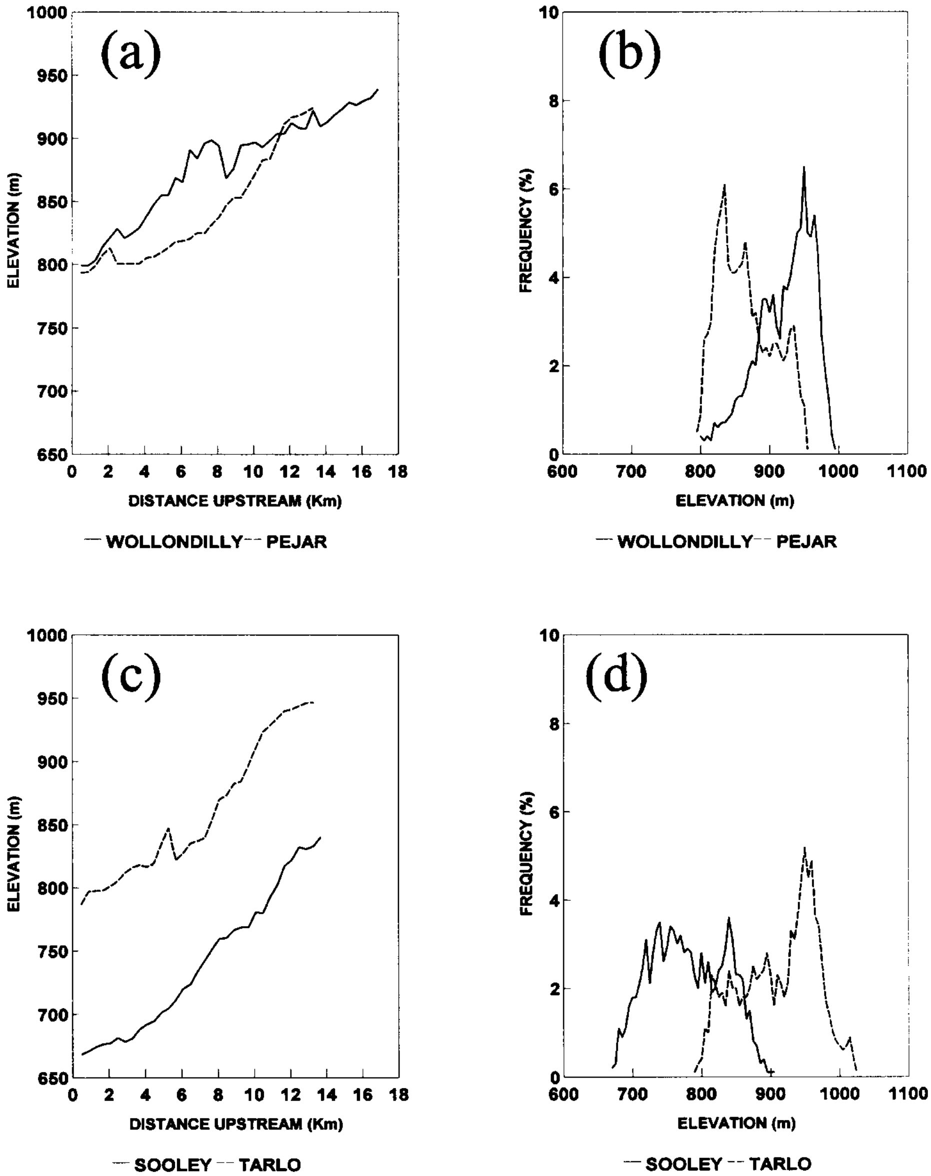

Figure 2. Topographic characteristics of the study catchments. Mean floodplain elevations with distance from catchment outlet for (a) the Wollondilly River and Pejar Creek, and (c) Sooley Creek (North) and Tarlo Creek. Frequency distribution of elevations for (b) the Wollondilly River and Pejar Creek, and (d) Sooley Creek (North) and Tarlo Creek

be masked in catchments where streams are not effective in removing delivered sediment, and there is a build-up of weathered and transported material extending uphill from valley floors and mantling even steep hillsides. Gradient analysis of gamma ray and slope data, stratified both by catchment and by lithology, has therefore been carried out to identify where systematic geological differences produce spurious relationships.

Relationships between slope and the distribution of K, Th and U for hillslopes in each of the four study catchments are shown in Figures 3, 4 and 5. K consistently increases with slope, as might be expected (see above), but the rate of increase seems to be greater in the steeper catchments. This may be the result of a build-up of weathered material on lower slopes in the less steep catchments because streams are not removing sediment (see below). There may also be an element of geological change in the pattern because a small area

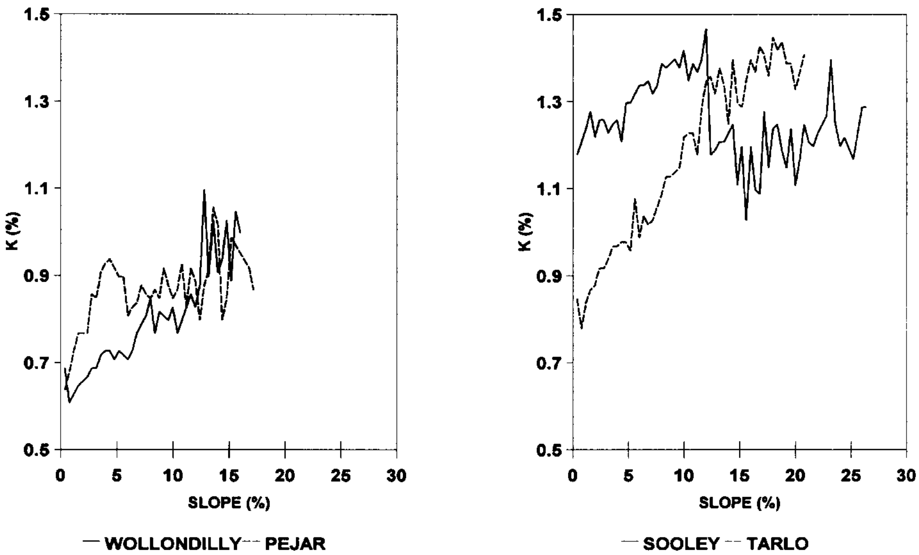

Figure 3. Mean K values for each slope category in the study catchments

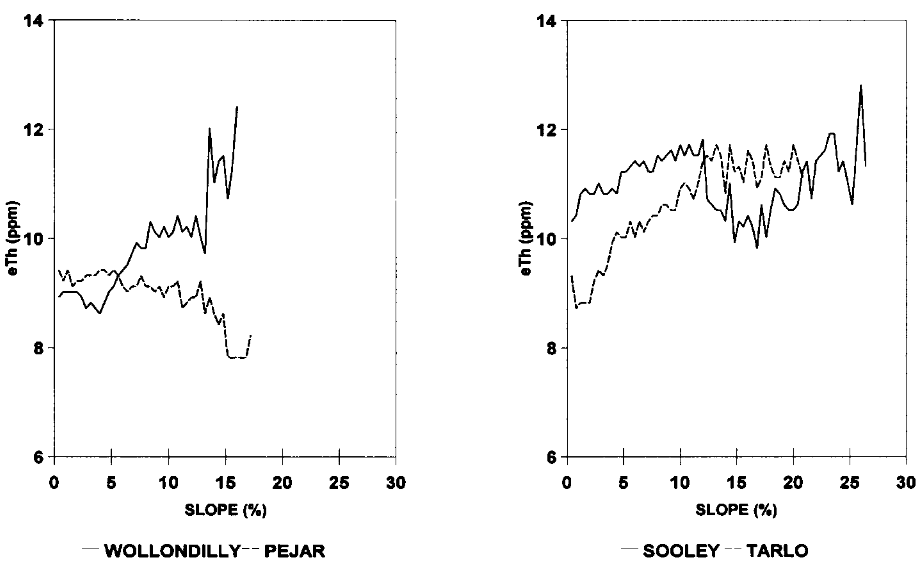

Figure 4. Mean eTh values for each slope category in the study catchments

of granite with a high K content is exposed in the lower reaches of Pejar Creek where slope is gentle. There is also a tendency for the relationship between K and slope to become irregular at slopes greater than about 12 per cent. This suggests that material does not accumulate in these steep areas, and that the gamma ray signal is derived from a mixture of fresh and weathered rock and residual soil. Observations in road cuttings in the area show that this is the case. The Th signal is similar to that of K except in the case of Pejar Creek where there is a gradual decrease in Th values with slope. This pattern may result from a build-up of sediment-bound Th on clay particles that have been retained on lower slopes. We investigate this further below. The U signal adds

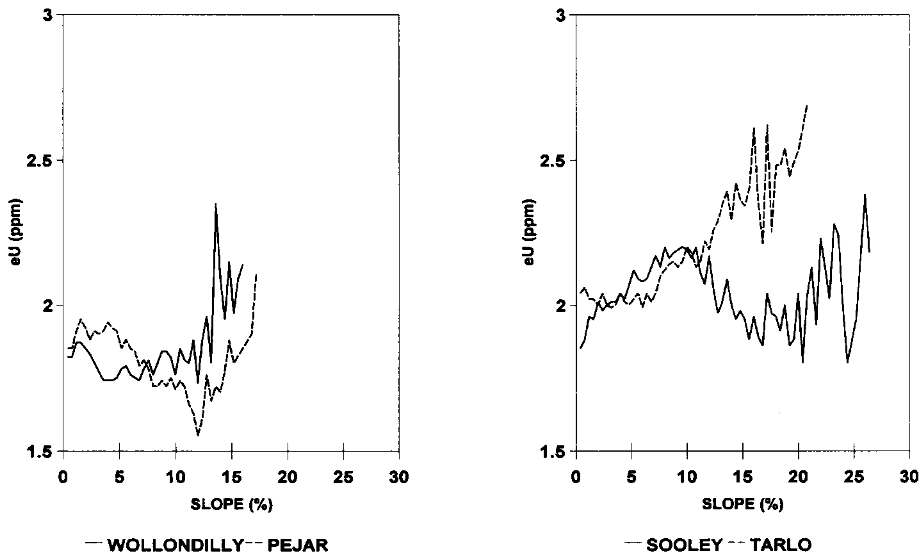

Figure 5. Mean eU values for each slope category in the study catchments

further complexity. On the Wollondilly River and Pejar Creek, there is a decrease in U with slope until the 12 per cent threshold is reached, after which U increases but in an irregular manner. Once again, we interpret the pattern of change above the 12 per cent slope cutoff as the effect of exposed rock and patchy regolith. However, the number of grid cells in each slope class above this value is very small and much less than what is required for gradient analysis where local variability is high (see Bastin *et al*, 1993). We may therefore be detecting this variability rather than underlying trends. Also, in the case of the Wollondilly, many of the lower slope values are associated with a basalt-capped plateau rather than occurring at the edge of the floodplain in the lower part of the catchment so the expected pattern of decreasing slope with lower elevation is reversed. On Sooley and Tarlo Creeks, U increases with slope up to the 12 per cent value, above which change becomes more irregular. This is similar to the pattern observed with K.

The conclusions derived from analysis by catchment are mostly confirmed when data are stratified by lithology. Relationships between slope and K, Th and U for granites, basalts and metamorphosed sediments are shown in Figure 6. K content is highest in the granites, lowest in the basalts and occupies the mid-range in the metamorphosed sediments. If we discount slopes greater than 10–12 per cent, where there are too few points for gradient analysis, K content increases with slope in all three lithologies, with the slowest rate of increase in the metamorphosed sediments. Th content behaves like that of K, except at low slopes, where the metamorphosed sediments have a higher Th content than the granites. We interpret this as both a weathering and sorting effect. U content is generally highest in the metamorphosed sediments followed by the granites and basalts. However, U varies inversely with slope in the granites and basalts but shows no trend in the metamorphosed sediments. The inverse relationship is probably due to both weathering and sorting.

We have suggested that some of the variations that occur in the relationships between slope and the gamma ray variables in the analysis by catchment may be a result of the position of steep and gentle slopes in the landscape. For example, do most of the gentle slopes occur on a plateau surface where the dominant process is *in-situ* weathering, or are they associated with plains in the lower reaches of the catchment where material has been deposited from upstream areas? Some of these issues may be resolved by comparing mean radiometric values with a spatial template describing distance upslope from the floodplain. In every case, K values show a U-shaped pattern in which there is an upslope decrease with distance from the floodplain followed by an increase (Figure 7). This pattern probably results from sediment sorting, with accumulation of clays and associated sediment-bound K in deposits on lower slopes, while the higher values in areas more distant from the floodplain are associated with exposed rock rather than depositional material. Beyond the U-shape, both

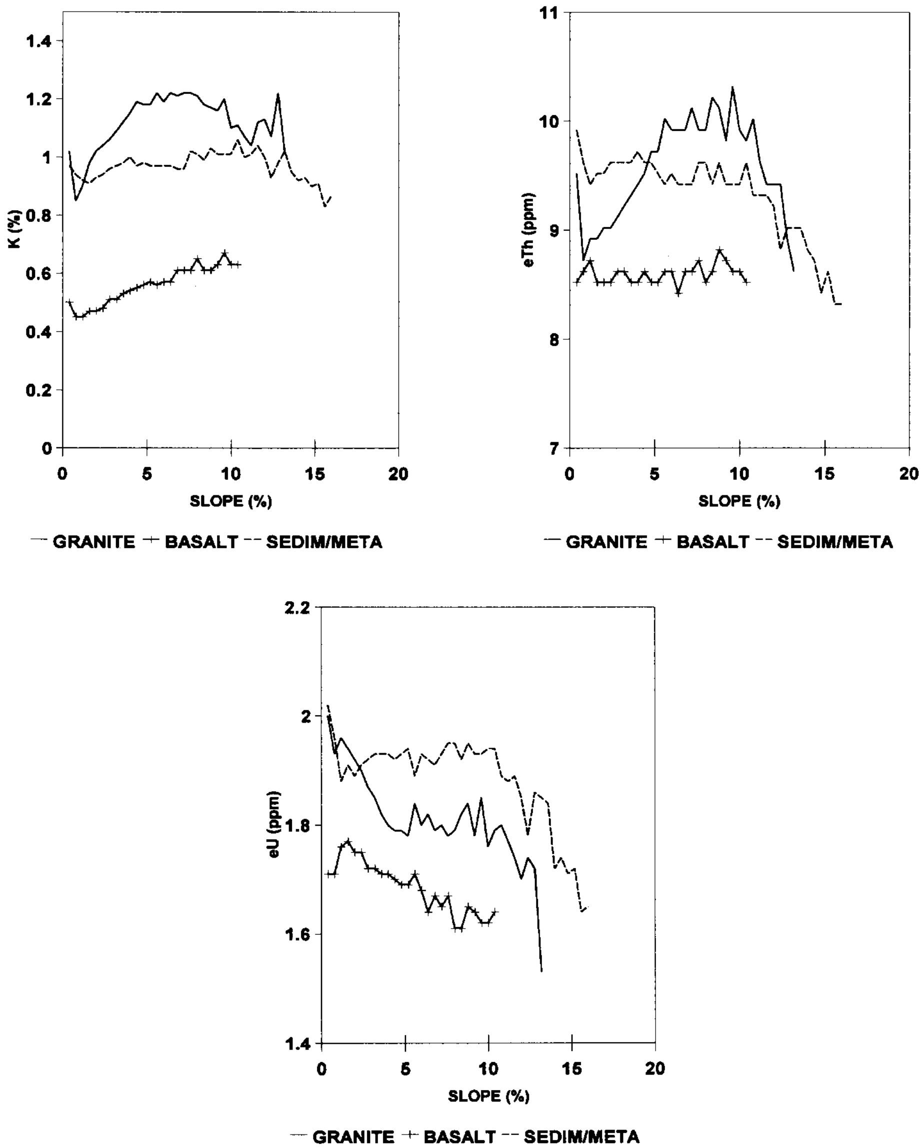

Figure 6. Variation in gamma ray values with slope for granite, metamorphosed sediments and basalt

the Wollondilly River and Pejar Creek show a sudden decrease in K with increasing distance from the floodplain. This appears to be the result of the basalt capping on the plateau surface. Th and U (not shown) behave in a similar manner to K.

Variations in radiometric response with upslope distance from the floodplain analysed by lithology are shown in Figure 8. The granites and metamorphosed sediments show decreasing K away from the floodplain. This effect is opposite to what might be expected since slopes tend to become steeper with distance from the floodplain until ridgetops are approached. The basalts show no apparent trend, perhaps because weathering reduces K content, offsetting the effect of sediment sorting. Th decreases away from floodplains in metamorphosed sediments, and to a lesser extent in granites, but there is little variation in the basalts. U consistently decreases with distance from the floodplain, as shown in the analysis by catchment.

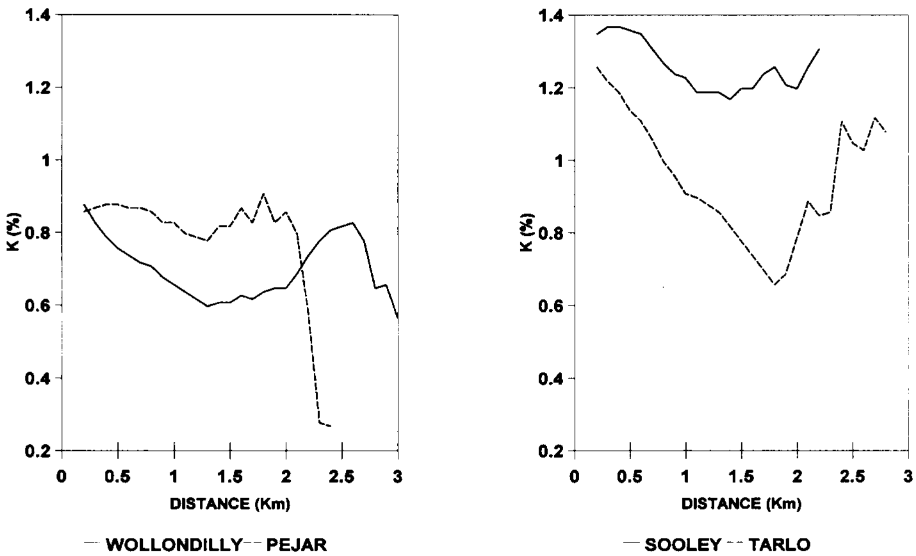

Figure 7. Mean K values on hillslopes with increasing distance from the floodplain in the study catchments

While there are strong relationships between slope, distance from the floodplain and the gamma ray variables, the situation with drainage area is less clear. In the case of K, Tarlo Creek and the Wollondilly show a weak log-linear or power relationship with drainage area while the other Pejar and Sooley Creeks show no relationship at all. The Th data display no obvious trend with drainage area, while the pattern of variation in U is inconsistent with any systematic trend with drainage area. A similar pattern emerges from analysis by lithological type. We interpret these patterns to mean that the influence of water erosion is limited, as might be expected in a landscape where transport processes are not particularly active, and the dominant activity is weathering. Alternatively, the effect of drainage area may be subsumed in the relationship between the gamma ray variables and slope since, on average, there is an inverse relationship between drainage area and slope. However, gradient analysis of the drainage area–radiometric variable relationship separately for gentle, medium and steep slopes does not indicate this.

Gamma radiometric patterns along stream channels and floodplains

Floodplains are usually sediment sinks, occur at relatively low slopes, and are frequently zones of sediment weathering, except in the most active landscapes, where floodplain sediments are in transit or floodplains are scoured down to bedrock. The gamma ray images show no evidence of simple trends in gamma ray emissions along flow paths which might indicate large volumes of sediment moving from hillslope source areas and along floodplains (see above). We therefore regard the floodplains as being relatively inactive and are looking for patterns of variation in K, Th and U associated with the presence or absence of deposited material, and with the past sorting and deposition of sediment load fractions.

Variations in gamma ray emissions along the floodplains are illustrated in Figures 9, 10 and 11 which show how these characteristics change with distance upstream of the catchment outlets. In the case of Pejar Creek, which has a gently sloping concave-upward long profile and a floodplain continuously filled with deposited material, K, Th and U all increase downstream except close to the catchment outlet where there is a sudden decline. The increase in gamma ray emissions probably results from progressively increasing clay content in floodplain sediments. The sudden decline occurs once water held in Pejar Dam is encountered. The Wollondilly River presents a more complicated picture. Beyond the 10 km point, where floodplain slopes are relatively gentle but there are a number of constrictions and openings (Figure 2), there is a general increase in Th and U but a highly variable K signal. We interpret this pattern as the result of a downstream increase in the

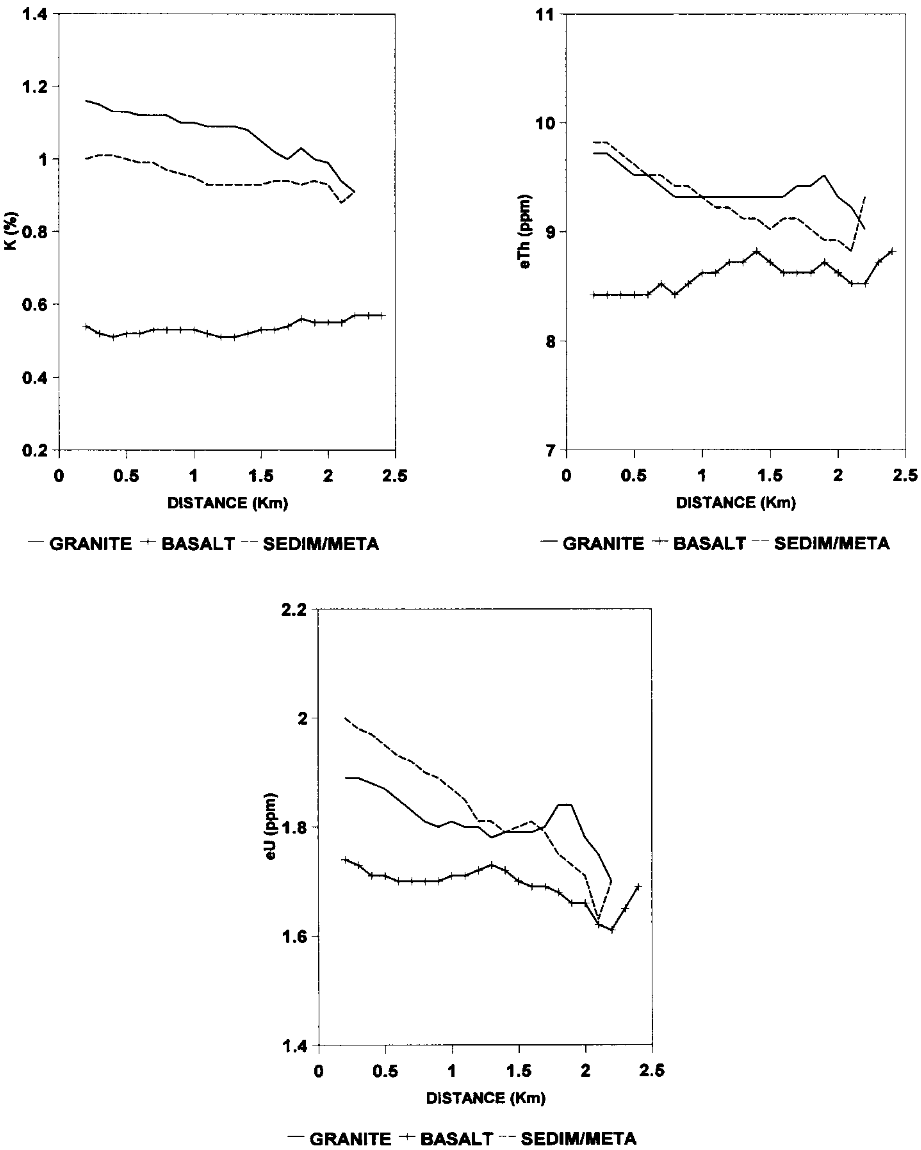

Figure 8. Variation in gamma ray values with increasing distance from the floodplain for granite, metamorphosed sediments and basalt

amount of finer sediments but, as field inspection shows, floodplain sediments are thin, and the amount of deposition varies between constrictions and openings producing local variations in gamma ray values. Downstream of the 10 km point, the Wollondilly River is confined in a steep and narrow valley with fresh granites exposed in constrictions and more weathered material surviving in valley openings. The fresh granite is associated with high K, Th and U values while lower values occur in valley openings, indicating the impact of weathering. Sooley and Tarlo Creeks both have steep long profiles and show substantial local variation in K and no downstream trend, as might be expected with valleys largely scoured down to bedrock. Th and U show a similar pattern suggesting that much of the variability arises because of local differences in exposed geology and the effect of valley openings and constrictions on the amount of weathered material present.

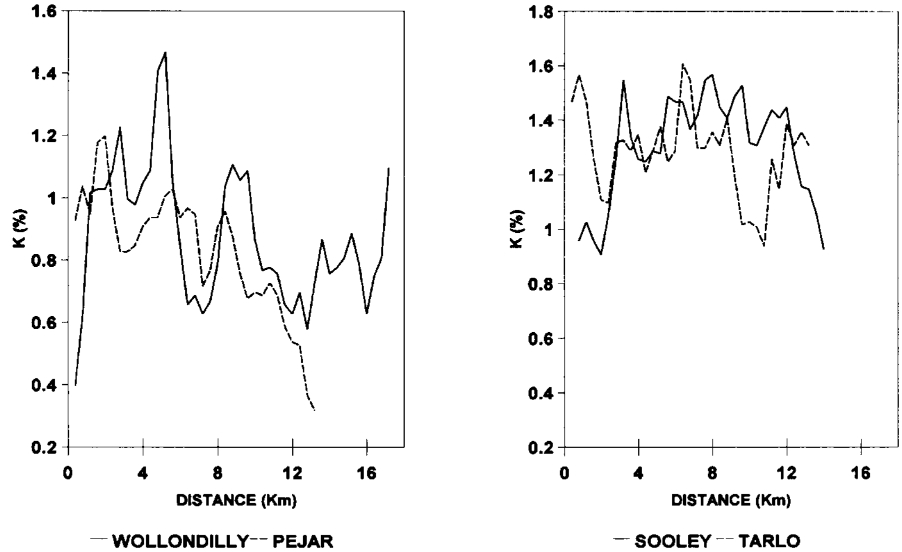

Figure 9. Downstream variation in mean K values along floodplains in the study catchments

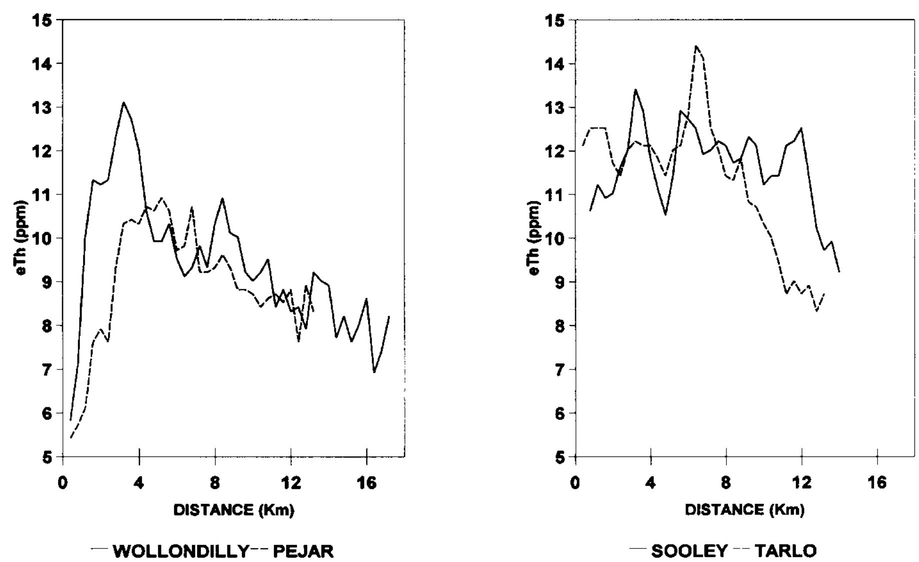

Figure 10. Downstream variation in mean eTh values along floodplains in the study catchments

Analysis of trends along floodplains by lithology was not feasible because streams cross too many different geological types.

Patterns associated with erosion/deposition models based on conservation of mass

Combining the slope and drainage area data for the four small catchments results in a linear relationship between slope and the various gamma ray variables together with a very weak power relationship for drainage

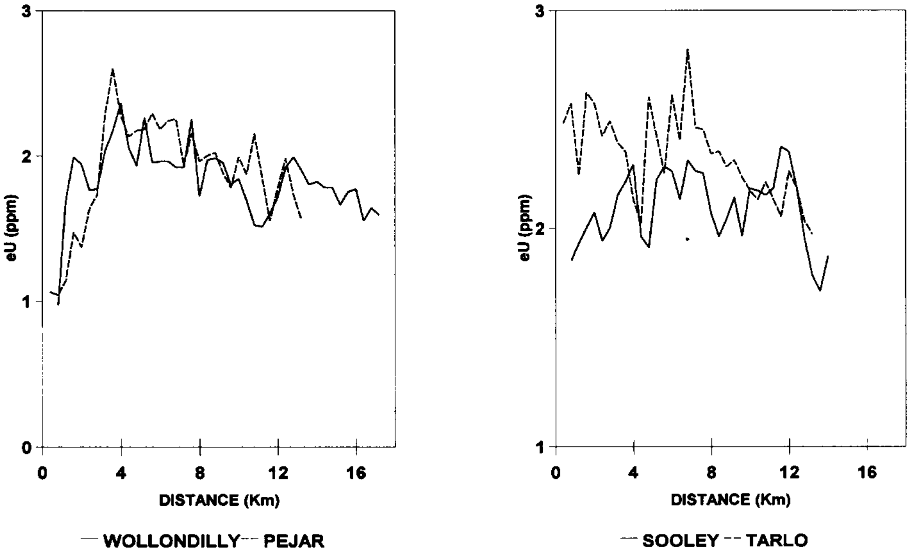

Figure 11. Downstream variation in mean eU values along floodplains in the study catchments

area (exponent values of 0·022 for K, 0·011 for Th and 0·004 for U). If we use these relationships as surrogate measures of sediment transport rate and substitute them into the appropriate conservation of mass equations, the resultant spatial templates can be compared with the individual gamma ray variables to determine whether gamma ray signature varies with the extent of erosion and deposition. Given the low values of the drainage area exponents, it makes little difference whether Equation 2 or 6 is used to provide the spatial template. The discussion that follows is based on the use of Equation 2 and a k value of 1·0, in which case positive values of the erosion equation indicate deposition, negative values suggest erosion, and values of zero imply no net gain or loss of sediment.

The gradient analysis results show virtually the same pattern in every case for the four catchments combined (Figure 12). All gamma ray variables have their highest values in areas of maximum deposition and show a decline as the amount of deposition decreases. A trough occurs in the zone of no net erosion or deposition followed by an increase in the gamma ray value as erosion becomes greater. This increase is only maintained over about half of the range of positive values of the conservation of mass equation. Beyond that, it becomes highly variable. We interpret the increase in gamma ray values with increasing deposition as the result of both selective deposition of finer particle sizes carrying sediment-bound K and accumulation of transported material. In eroding areas, the increase in gamma ray values results from the exposure of progressively less weathered rock as erosion intensity increases. Eventually, however, a point is reached where very little regolith survives and local variations in underlying geology dominate the pattern.

Repeating the analysis with gamma ray data stratified by lithology (Figure 13) yields patterns of change in granites and metamorphosed sediments similar to those observed for the combined catchments. Absolute gamma ray values are different for each rock type but the inflection point in the curves corresponding to no net erosion or deposition is always present. The trends in gamma ray values with increasing erosion and deposition intensity are also similar. These patterns are clearly not generated by lithological differences. The basalt data do not behave in the same way. The K shows the normal U-shape centred on erosion equation values of zero but the pattern is inverted for both Th and U. This change is unexpected given that both weathering and accumulation of clays in deposition areas on basalts should lead to elevated Th and U signals (see Dickson *et al*, 1996). Further examination of data shows very few areas on the basalt with erosion equation values greater than zero. The inverted pattern is produced by only three grid cells which is not

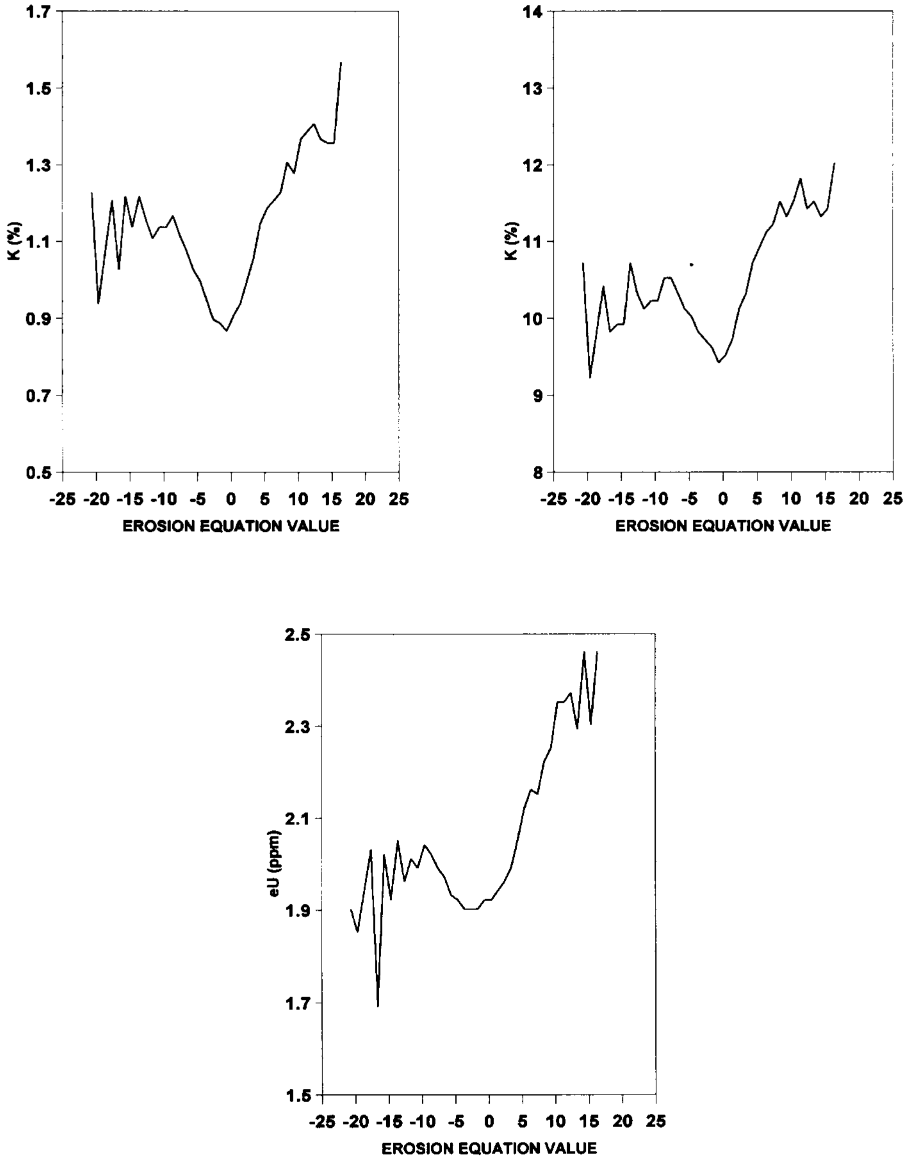

Figure 12. Variation in mean gamma ray values with the extent of erosion and deposition as determined using Equations 1 and 2

enough for gradient analysis. We therefore conclude that it is due to local variability and a small sample rather than a real difference in behavioural trend.

DISCUSSION

It is clear from the results that data acquired from airborne gamma ray remote sensing contain patterns of spatial variation which can be related to common topographic indicators of sediment transport rate, of downstream sorting of sediments, and of the extent and location of erosion and deposition. The data may also provide indications of the pattern of weathering in areas where there is no obvious deposition. This raises the

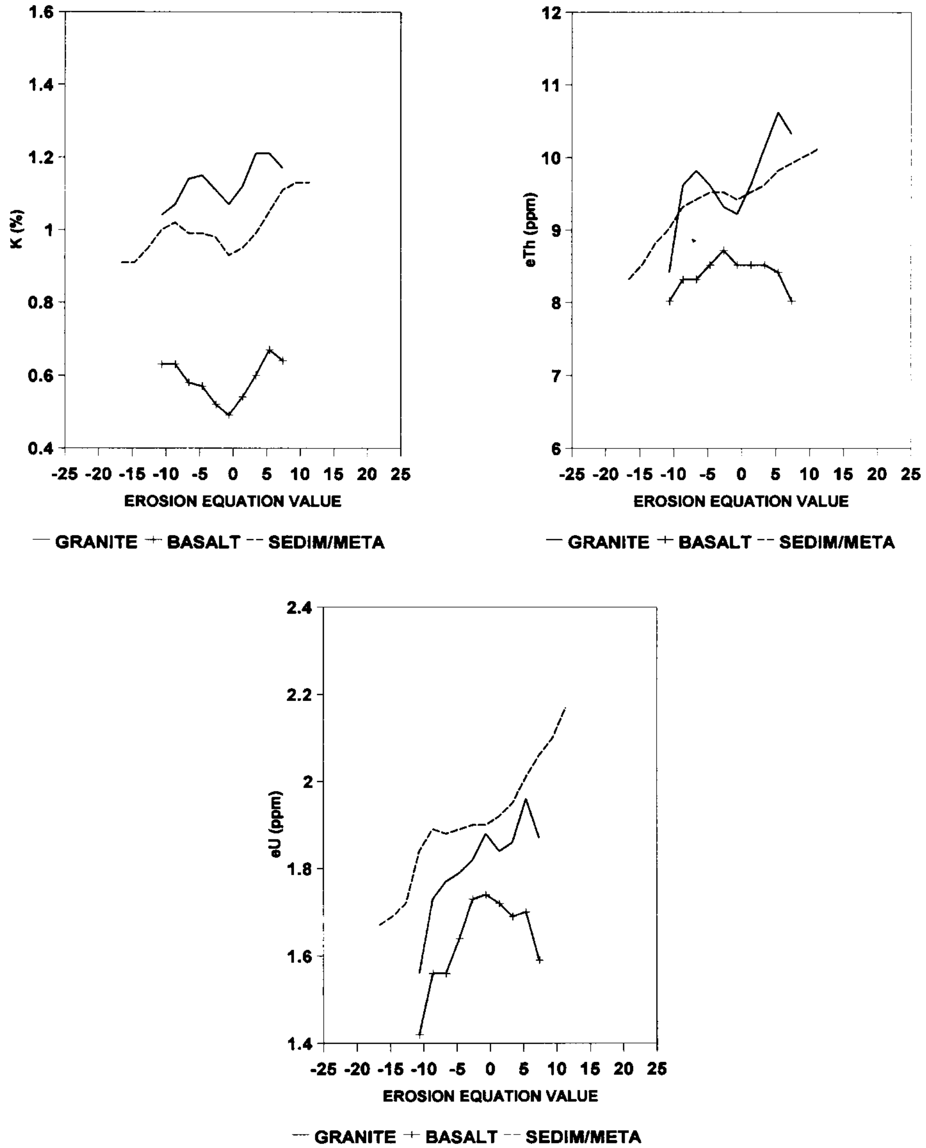

Figure 13. Variation in mean gamma ray values with the extent of erosion and deposition as determined using Equations 1 and 2 for granite, metamorphosed sediments and basalt

possibility of using gamma ray signatures as indicators of the location and the relative, if not absolute, extent of erosion and deposition.

We see two potential applications. Firstly, when gamma ray data are used in geological survey, it may be difficult to separate spatial patterns due to weathering and transport of material from those associated with changes in lithology or mineralogy. Gradient analysis and the use of spatial templates based on geomorphic process models offer a way of resolving these ambiguities. Secondly, and of more interest to geomorphologists, is the possibility of calibrating models of long-term sediment transport rate and erosion and deposition using the gamma ray signatures of eroded and depositional surfaces. This would allow verification of regional-scale process models and increase our ability to work at the whole catchment or landscape scale.

A number of problems still need to be solved if the capacity to calibrate sediment transport models is to be developed. It is also necessary to recognize the limitations imposed by the spatial resolution of gamma ray data collected from aircraft. The problems include the need for greater capability to distinguish between the gamma ray patterns generated by erosion and deposition and those that arise from local variations in geology. There is also a need to know more about the nature of gamma ray signatures in deposition areas and to distinguish between the effects of selective deposition of finer sediments and the impact of weathering. At present, we are only able to infer differences between these processes because of an association with topographic patterns. More is needed if results are to be more definitive.

We see several ways forward. Firstly, where geology is relatively uniform and there is good quality mapping, it should be possible to construct explicit models of how gamma radiometric signatures change as the extent of weathering increases. One approach might be to segment the landscape into areas of bare, relatively unweathered rock based on steepness of slope and values of the conservation of mass equation. These areas might provide a gamma ray signature for fresh rock that will be modified as the amount of weathering increases. As slope decreases and as the value of the conservation of mass equation moves towards no net erosion, a greater proportion of weathered material is likely to occur in the regolith and the associated gamma radiometric changes indicate the effects of weathering. Where geology is more complex or remains unknown, this approach is likely to be less successful although the effects of weathering may not be unique to a particular rock type, allowing considerable generalization.

In areas of deposition, gamma ray signatures may be unrelated to the underlying rock. However, they will be a function of the source material, the degree of sorting and the amount of weathering. Deposition areas can be identified using the conservation of mass equation and analysed separately from eroded areas. In landscapes where sediment transport is currently active, the gamma radiometric characteristics of deposited material should closely reflect those of material being eroded from the upslope area. Where sediment transport has largely ceased, the similarity may be progressively reduced over time by weathering. The extent to which gamma radiometric signatures in a given location reflect those of material upslope can be estimated by accumulating each type of source material down the flow path and calculating the proportion or total amount of material contributed from the different upslope environments at each location. The amount of material contributed from each upslope grid cell can be a constant or can be made dependent on parameters such as slope, amount of vegetation cover, calculated transport rate, a soil-erodibility constant, or a combination of these. Also, non-contributing parts of the landscape may be masked out during the process. A modified version of the flow path identification and drainage accumulation routine of the DRM previously developed by Pickup and Chewings (1996) allows this type of analysis and will be used in the next stage of our work.

Separating the effects of sediment sorting from weathering remains a problem. In the study area, it seems that progressive accumulation of finer material increases K signals in all three lithologies and increases Th signals in the granites and metamorphosed sediments. The presence of more weathered material means lower K and higher U signatures in granites and basalts but little change in the metamorphosed sediments. Dust mantles may also have some effect on both weathering and sorting patterns (Dickson and Scott, 1998). At present, we have no direct solution to this problem. However, it may be that the use of ancillary data such as mineralogical maps derived from analysis of data from Landsat Thematic Mapper (e.g. Dickson *et al.*, 1996) or from aircraft-mounted hyperspectral sensors may offer opportunities.

While airborne geophysical data seems to offer considerable possibilities for large-scale erosion and deposition mapping, there are also limitations. In Australia, most data are acquired at a line spacing of 200 m or 400 m although more detailed surveys have been carried out in areas with mineral prospects. Elevation data along survey lines are more closely spaced but there is a limit to the DEM grid cell size that can be generated because of the need to interpolate between lines. The grid cell size of 100 m used in this paper is a reasonable compromise between loss of information on terrain characteristics because of the smoothing associated with larger grid cells and the generation of artifacts by the interpolation routines used in DEM generation as grid cells become smaller. Even so, as Gessler (1996) has shown, there is a considerable loss of capacity to predict soil characteristics from terrain as grid cell size becomes greater than 80 m. Indeed, much

of the local variability in both terrain characteristics and soil properties requires a grid cell spacing of 10 m or less to be captured fully. Clearly, the airborne data are best used to resolve general trends in erosion and deposition across the landscape.

The gamma ray data are less prone to errors arising from spatial interpolation since they already represent spatial averages. In fact, they may introduce too much spatial smoothing to distinguish many of the local variations in soil properties. Also of concern are the quantization levels that can be achieved at commonly used flying heights and speeds. Both Th and U data have a significantly lower level of accuracy than K data and, while ratioing of gamma ray variables has proved effective when using stream sediments as environmental tracers (Olley, 1994), ratioing of airborne data has an adverse effect on signal to noise ratio. Indeed ratios show no clear relationship with terrain characteristics. Once again, it seems that the data that are available from airborne survey are only adequate for the identification of general trends.

CONCLUSIONS

While gamma radiometric data from airborne geophysical surveys are largely determined by lithology and, to a lesser degree, weathering, they have a role to play in the regional-scale erosion modelling. They offer surrogate information on the intensity and location of erosion and deposition but extraction of this information requires ancillary data on topography. The survey data also provide information on elevation that may be used to construct digital elevation models. Gradient analysis techniques may be used to extract information on the relationship between topographic characteristics and gamma ray signatures and this relationship may be interpreted in geomorphic process terms. Such information can help resolve whether particular spatial patterns in gamma ray are due to differences in underlying geology or whether they result from surficial transport and weathering.

The ability to recognize transport processes raises the possibility of using gamma ray data to design and calibrate regional-scale sediment transport models. Currently used sediment tracing technology is expensive and provides point data for a few locations rather than the spatially distributed information which is really needed. Our success in identifying transport-related patterns in a landscape dominated by geological differences and weathering effects is sufficiently encouraging to apply the technique in other areas. Indeed, a subsequent paper (G. Pickup and A. Marks, submitted for publication in *Earth Surface Processes and Landforms*, 1999) will show that sediment sources, sinks and flow paths can be extracted from gamma ray data in landscapes where landscape development is dominated more by transport than by weathering.

ACKNOWLEDGEMENTS

We wish to thank John Finnigan, Bruce Dickson, Steve Billings, Brian Minty, Jon Olley and Ian Prosser for discussions, advice, assistance in deriving models, and processing of data. Gary Caitcheon and Jon Olley provided geophysical survey data and encouraged us to explore possibilities of identifying erosion and deposition patterns related to terrain characteristics. Vanessa Chewings was responsible for much of the coding of the gradient method.

REFERENCES

Anderson MG. 1988. Modelling Geomorphological Systems. John Wiley & Sons: Chichester.

Aspin SJ, Bierworth PN. 1997. GIS analysis of the effects of forest biomass on gamma-radiometric images. Third National Forum on GIS in the Geosciences. *Australian Geological Survey Organisation Record* **1997/36**: 77–83.

Bastin GN, Pickup G, Chewings VH, Pearce G. 1993. Land degradation assessment in central Australia using a grazing gradient method. *Rangeland Journal* **15**: 190–216.

Bauer J. 1988. User's Guide to the Digital Relief Model. Department of Physical Geographic and Landscape Ecology, Technical University Braunschweig.

Bierworth P. 1996. Investigation of airborne gamma-ray images as a rapid mapping tool for soil and land degradation - Wagga Wagga, NSW. *Australian Geological Survey Organisation Record* **1996/22**.

Caitcheon GG. 1993. Sediment source tracing using environmental magnetism: a new approach with examples from Australia. *Hydrological Processes* **7**: 349–358.

Chow VT. 1959. Open-Channel Hydraulics. McGraw-Hill Book Company: New York.

Clark DA. 1997. Magnetic petrophysics and magnetic petrology: aids to geological interpretation of magnetic surveys. *Australian Geological Survey Organisation Journal of Australian Geology and Geophysics* **17**: 83–104.

Cook SE, Corner RJ, Groves PR, Grealish GJ. 1996. Use of airborne gamma radiometric data for soil mapping. *Australian Journal of Soil Research* **34**: 183–194.

Croke J, Hairsine PB, Fogarty P. (in press). Sediment production, storage and redistribution on logged hillslopes.

Denham D. 1997. Airborne geophysics in Australia: the Government contribution. *Australian Geological Survey Organisation Journal of Australian Geology and Geophysics* **17**: 3–10.

Dickson BL, and Scott KM. 1992. Interpretation of Aerial Gamma-Ray Surveys. CSIRO Division of Exploration Geoscience Restricted Report 301R. North Ryde.

Dickson BL, Fraser SJ, Kinsey Henderson A. 1996. Interpreting aerial gamma-ray surveys utilising geomorphological and weathering models. *Journal of Geochemical Exploration* **57**: 75–88.

Dickson BL, Scott KM. 1997. Interpretation of aerial gamma-ray surveys –adding the geochemical factors. *Australian Geological Survey Organisation Journal of Australian Geology and Geophysics* **17**: 187–200.

Dickson BL, Scott KM. 1998. Recognition of aeolian soils in the Blayney district, NSW: implications for mineral exploration. *Journal of Geochemical Exploration* **63**: 237–251.

Felton EA. 1974. Goulburn 1:250,000 Metallogenic Map. Geological Survey of New South Wales: Sydney.

Flanagan DC, Nearing MA. 1995. USDA - Water Erosion Prediction Project: Hillslope profile and watershed model documentation NSERL Report 10. USDA-ARSNSERL: West Lafayette, Indiana.

Galbraith JH, Saunders DF. 1983. Rock classification by characteristics of aerial gamma-ray measurements. *Journal of Geochemical Exploration* **18**: 49–73.

Gessler P. 1996. Statistical Soil–Landscape Modelling for Environmental Management. PhD thesis. Australian National University.

Grasty RL. 1975. Atmospheric absorption of 2·62 MeV gamma ray photons emitted from the ground. *Geophysics* **40**: 1058–1065.

Grasty RL. 1979. Gamma ray spectometric methods in uranium exploration –theory and operational procedures. In Geophysics and Geochemistry in the Search for Metallic Ores, Hood PJ, (ed.). *Geological Survey of Canada, Economic Geology Report* 31. 147–161.

Grasty RL, Minty BRS. 1995. A guide to the technical specifications for airborne gamma ray surveys. *Australian Geological Survey Record* **1995/60**.

Grayson RB, Argent RM, Nathan RJ, McMahon TA, Mein RG. 1996. Hydrological Recipes. Estimation Techniques in Australian Hydrology. Cooperative Research Centre for Catchment Hydrology: Melbourne.

Hird C. 1991. Soil Landscapes of the Goulburn 1: 250,000 sheet. Soil Conservation Service of New South Wales: Sydney.

Horsfall KR. 1997. Airborne magnetic and gamma-ray data acquisition. *Australian Geological Survey Organisation Journal of Australian Geology and Geophysics* **17**: 23–30.

Kirkby MJ. 1987. Modelling some influences of soil erosion, landslides and valley gradient on drainage density and hollow development. In Geomorphological Models. Theoretical and Empirical Aspects, Ahnert F (ed.). *Catena Supplement* **10**: 1–14.

Kirkby MJ. 1995. Modelling the links between vegetation and landforms. *Geomorphology* **13**: 319–335.

Kirkby MJ, Imeson AC, Bergkamp G, Cammeraat LH. 1996. Scaling up processes and models from the field plot to the watershed and regional areas. *Journal of Soil and Water Conservation* **51**: 391–396.

Loughran RJ. 1984. Studies of suspended sediment transport in Australian drainage basins –a review. In Drainage Basin Erosion and Sedimentation, Loughran RJ (ed.). University of Newcastle: New South Wales; 139–146.

Luyendyk APJ. 1997. Processing of airborne magnetic data. *Australian Geological Survey Organisation Journal of Australian Geology and Geophysics* **17**: 31–38.

Minty BRS. 1997. Fundamentals of airborne gamma-ray spectrometry. *Australian Geological Survey Organisation Journal of Australian Geology and Geophysics* **17**: 39–50.

Minty BRS, MacFadden PL. 1998. Improved NASVD smoothing of airborne gamma ray spectra. *Exploration Geophysics* **29**: 516–523.

Minty BRS, Luyendyk APJ, Brodie RC. 1997. Calibration and data processing for airborne gamma-ray spectrometry. *Australian Geological Survey Organisation Journal of Australian Geology and Geophysics* **17**: 51–62.

Nearing MA, Lane LJ, Alberts EE, Laflen JM. 1990. Prediction technology for soil erosion by water: status and research needs. *Soil Science Society of America Journal* **54**: 1702–1711.

Olley JM. 1994. The Use of ^{238}U and ^{232}Th Decay Series Radionuclides in Sediment Tracing. PhD thesis. University of New South Wales.

Olley JM, Murray AS, MacKenzie DH, Edwards K. 1993. Identifying sediment sources in a gullied catchment using natural and anthropogenic radioactivity. *Water Resources Research* **29**: 1037–1043.

Ong C, Hick P. 1998. Final Report. Quantitative Remote Sensing of Environmental Impacts at Ranger Mine. Report from CSIRO Minesite Rehabilitation Research Program for ERAES. CSIRO Division of Exploration and Mining Report 522c; 1–61.

Pickup G, Chewings VH. 1986. Random field modelling of spatial variations in erosion and deposition in semi-arid central Australia. *Ecological Modelling* **33**: 269–296.

Pickup G, Chewings VH. 1994. A grazing gradient approach to land degradation assessment in arid areas from remotely sensed data. *International Journal of Remote Sensing* **15**: 597–617.

Pickup G, Chewings VH. 1996. Effects of topography on plant cover and erosion under grazing in arid rangelands. *Earth Surface Processes and Landforms* **21**: 517–529.

Rieger WA, Olive LJ. 1988. Channel sediment loads: comparisons and estimations. In Fluvial Geomorphology of Australia, Warner RF (ed.). Academic Press: Sydney; 69–85.

Ritchie JC, McHenry JR. 1990. Application of radioactive fallout caesium-137 for measuring soil erosion and sediment accumulation rates and patterns: a review. *Journal of Environmental Quality* **19**: 215–233.

Schwarz GF, Klingele EE, Rybach L. 1992. How to handle rugged topography in airborne gamma ray spectrometry surveys. *First*

Break **10**: 11–1.

Walden J, Slattery MC, Burt TP. 1997. Use of mineral magnetic measurements to fingerprint suspended sediment sources: approaches and techniques for data analysis. *Journal of Hydrology* **202**: 353–372.

Wallbrink PJ, Murray AS, Olley JM, Olive LJ. 1998. Determining sources and transit times of suspended sediment in the Murrumbidgee River, New South Wales, Australia, using fallout ^{137}Cs and ^{210}Pb. *Water Resources Research* **34**: 879–887.

Walling DE. 1983. The sediment delivery problem. *Journal of Hydrology* **65**: 209–237.

Wasson RJ, Olive LJ, Rosewell CJ. 1996. Rates of erosion and sediment transport in Australia. Erosion and Sediment Yield: Global and Regional Perspectives. International Association for Hydrological Sciences Publication **236**;139–148.

Wilford J. 1995. Airborne gamma-ray spectrometry as a tool for assessing relative landscape activity and weathering development of regolith, including soils. *Australian Geological Survey Organisation Research Newsletter* **22**: 12–14.

Wilford J, Bierworth PN, Craig MA. 1997. Application of airborne gamma-ray spectrometry in soil/regolith mapping. *Australian Geological Survey Organisation Journal of Australian Geology and Geophysics* **17**: 201–216.

Willgoose GR, Bras RL, Rodriguez-Iturbe I. 1991. A physically based coupled network growth and hillslope evolution model: 1 Theory. *Water Resources Research* **27**: 1671–1684.

Wischmeier WH, Smith DD. 1978. Predicting Rainfall Erosion Losses, a Guide to Conservation Planning. Agricultural Handbook No. 537. US Department of Agriculture: Washington DC.